

Collisions in a System of Conical Jet/Counterjet Outflows

A. C. Raga[†] \mathbb{O}^1 , Z. Meliani \mathbb{O}^2 , A. Rodríguez-González \mathbb{O}^1 , S. Cabrit \mathbb{O}^3 , G. Pineau des Forêts \mathbb{O}^3 , J. I. Castorena \mathbb{O}^1 and A. Esquivel \mathbb{O}^1

Keywords: ISM: jets and outflows, ISM: kinematics and dynamics, stars: pre-main sequence, stars: winds, outflows

Abstract

Stars predominantly form in compact, non-hierarchical clusters. The gas outflows ejected by protostars can intersect and interact with each other, resulting in complex interactions that affect the dynamics, morphology, and evolution of these outflows. Determining the probability of an encounter between them requires a Bayesian approach that considers the collimation, length (or age), and separation between young stellar objects in clusters. In this study, we employed a Monte Carlo approach to estimate this probability as a function of the jet opening angle and the ratio between the jet length and separation between stars. We propose a function that predicts the number of interactions within a cluster based on the opening angle of the gas outflows ejected by protostars.

Resumen

Las estrellas se forman, predominantemente, en cúmulos compactos. Los flujos de gas eyectados por proto-estrellas pueden cruzarse e interactuar entre sí, lo que resulta en una compleja interacción. Estas interacciones afectan la dinámica, morfología y evolución de estos flujos. La determinación de la probabilidad de encuentro entre ellos requiere un enfoque bayesiano que considere la colimación, longitud (o edad), la separación entre objetos estelares jóvenes en cúmulos. En este estudio, empleamos un enfoque de Monte Carlo para estimar esta probabilidad como función del ángulo de apertura del chorro y la relación entre la longitud del chorro y la separación entre estrellas. Proponemos una función que predice el número de interacciones dentro de un cúmulo basada en el ángulo de apertura de los flujos de gas eyectados por protoestrellas.

Corresponding author: Ary Rodríguez González E-mail address: ary@correo.nucleares.unam.mx

Received: December 17, 2024 Accepted: September 17, 2025

1. Introduction

The interaction of molecular outflows is a fascinating phenomenon for understanding the early evolution of low-mass stellar objects in star-forming regions. Low-mass objects are formed through an accretion process, resulting in the production of collimated outflows that eject material from very close to the formed object, known as astrophysical jets.

In Nony et al. (2020), the mass structure of the complex W43 cloud was studied, focusing on pre-stellar and protostellar objects in this mini-starburst phase. They found that 51 out of 127 cores in the cloud were associated with molecular outflows, whereas some lacked associated outflows. These numerous objects are located within a filamentary structure approximately 1 pc long along its major axis. The high probability of collision and interaction between the molecular outflows in this region is evident from ALMA telescope images in CO (2-1) (see Fig. 2 in Nony et al. 2020).

Similar interactions between molecular outflows have been previously reported in association with BHR71, which exhibits a pair of outflows emanating from two young protostars within a Bok globule. The outflows in BHR 71 interact with the surrounding material in the molecular cloud, causing shock waves and gas compression. These molecular outflows are likely colliding, as indicated by an increase in the brightness of the CO emission, the velocity dispersion in the impact zone, and change in the orientation of one of the outflows (IRS 2; Zapata et al., 2018).

More recently, in Cep E-south, a cavity was observed in the envelope of the main jet due to a perpendicular secondary jet interacting with it, destroying molecules primarily in CO (2-1) emission (see Lefloch et al. 2018). Furthermore, Rodríguez-González et al. (in prep.) demonstrated that this interaction of molecular outflows drastically changes the structure of the envelopes associated with jets from Class 0/I objects.

In this study, we aim to estimate the probability of such interactions occurring and how this is related to their separation distance and opening angle. The remainder of this paper is organized as follows: In § 2, we calculate the probability of interaction between two conical flows as a function of their opening angles and the distances each travels. The extension to a system with more than one jet is explored in § 3. We make

¹Instituto de Ciencias Nucleares, UNAM, México.

²LUTH, Observatoire de Paris, CNRS, PSL, Université de Paris; 5 Place Jules Janssen, 92190 Meudon, France.

³Observatoire de Paris, PSL University, Sorbonne University, CNRS, LERMA, 75014 Paris, France.

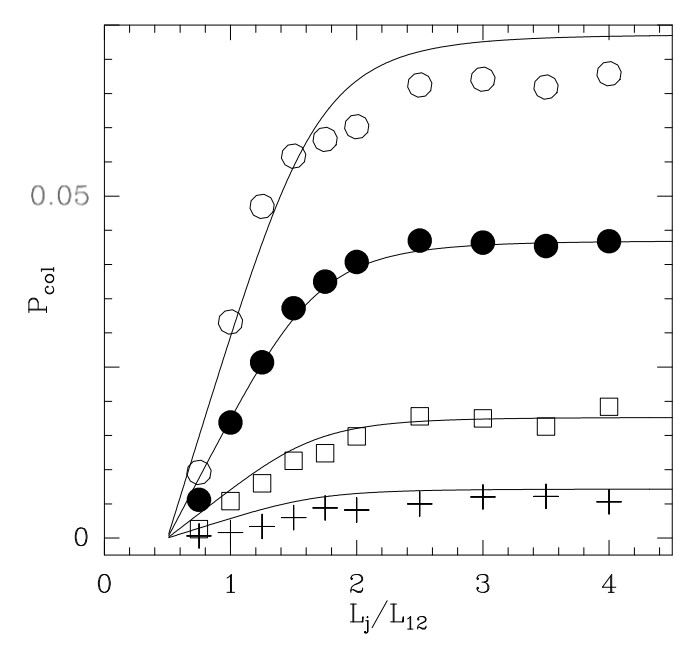


Figure 1. The probability of collision between two "double cone" outflows as a function of the L_j/L_{12} jet length to source separation ratio. The results of sets of 10^4 "Bernoulli experiments" for double cones with half-opening angles $\alpha=2.5^\circ$ (crosses), 5° (squares), 10° (full circles) and 15° (open circles) are shown. The solid curves are obtained from the analytic fit of equation (1) for the same α values.

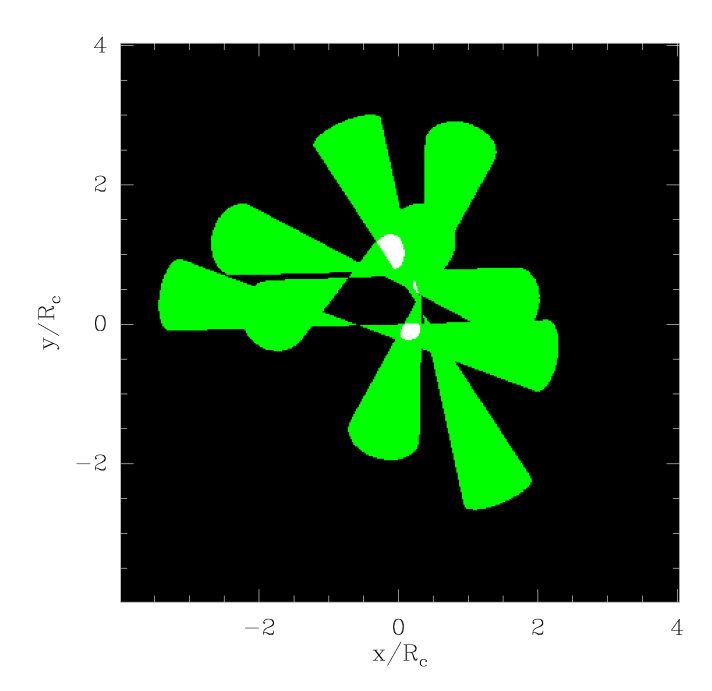


Figure 2. Configuration of a system of $N_j=5$ biconical bipolar outflows with a half-opening angle $\alpha=10^\circ$. The outflow directions are randomly chosen, and the source positions are obtained by sampling a uniform source distribution within a sphere of radius R_c . The projection of the cones on the xy-plane is shown in green, and the regions of physical (3D) superpositions between cones are shown in white. The outflow cones have $L_j=3R_c$ lengths.

theoretical assumptions to test our approximations, which are detailed in § 4. The experiments based on gas dynamics are described in § 5. § 6 is dedicated to applying our models to predict

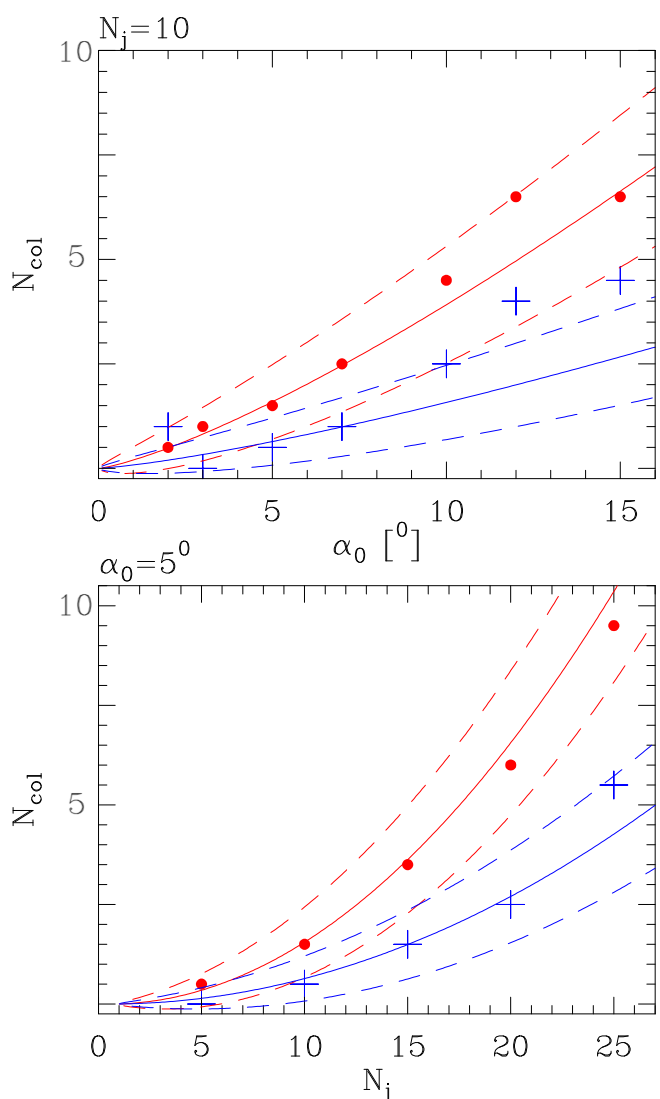


Figure 3. Top: Number of jet superpositions as a function of the half-opening angle α for a system of $N_j=10$ bi-conical outflows. The results for (single) Bernoulli experiments of randomly directed jets from sources with a uniform spatial distribution within a sphere of radius R_c have been computed for cones of length $R_j=R_c$ (blue crosses) and $R_j=3R_c$ (red circles). The solid curves correspond to the results obtained with the analytic fit of equation (3), and the dashed curves are the corresponding $\pm \sigma$ envelopes. Bottom: number of jet superpositions for a system of cones with $\alpha=5^\circ$ as a function of the number N_j of jets with sources within a sphere of radius R_c . The results for jets of lengths $R_j=R_c$ (blue crosses and curves) and $R_j=3R_c$ (red circles and curves) are shown.

the interacting conical flows. Finally, we present the conclusions of our study in the last section of the paper.

2. Interaction between two outflows

We first consider a problem of two jet/counterjet, conical outflows of half-opening angle α and length L_j (measured from the source to the tip of the jet or the counterjet), with a separation L_{12} between the two sources. To evaluate the probability p of having a physical collision between the two outflows, we carry out a Montecarlo simulation of N "Bernoulli experiments" in which the orientations of the two outflows are chosen randomly, and we count the number N_c of cases which lead to a collision between the

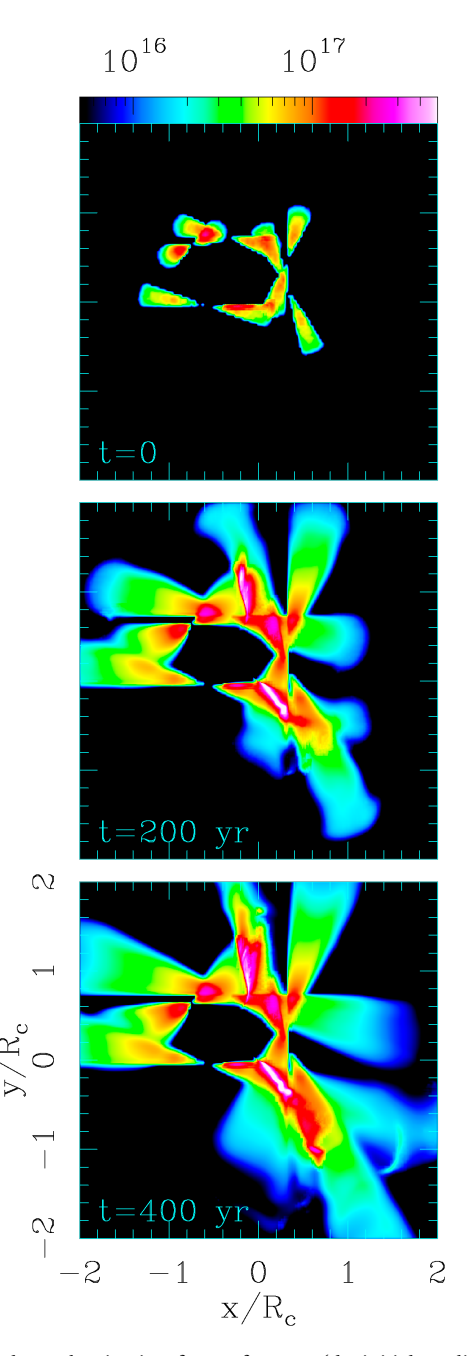


Figure 4. Column density time frames for t=0 (the initial condition, top frame), 200 (center) and 400 yr time-integration (bottom) obtained from the 3D gasdynamic simulation described herein. The column densities are displayed with the logarithmic scale given (in cm⁻² by the top bar). The column densities correspond to integrations along the *z*-axis, and the (x,y) coordinates are given in units of the $R_c=5\times 10^{16}$ cm radius of the outflow source position distribution. The source position and direction values for the 5 bipolar outflows are the same as the ones of the geometrical model of Figure 2.

lobes of the two outflows. The simulation then gives an estimate $P_{col}=N_{col}/N$ for the two-outflow collision probability.

The collision probability P_{col} as a function of the jet length to source separation ratio L_j/L_{12} (obtained from simulations with $N=10^4$ experiments) is shown in Figure 1. The probability is given for four values of the half-opening angle of the outflow cones: $\alpha=2.5$, 5, 10 and 15°.

As expected, the collision probability P_{col} is zero for $L_j/L_{12} \le 1/2$ (since this condition implies that the outflows never touch). For $L_j/L_{12} > 1/2$, p first grows and then reaches an approximately constant limit $L_j/L_{12} > 2.5$ (see Figure 1).

Also, in Figure 1, it is clear that the collision probability p is a growing function of the half-opening angle α . We propose a form $P_{col} \propto \alpha^q$. For small opening angles:

- in perpendicular jet collisions, the solid angle subtended by the obstructing jet is $\propto \alpha$, so we would expect $q \approx 1$,
- in collisions of closely aligned jets, the solid angle of the obstructing jet is ∝ α², giving q ≈ 2.

We find that a q=1.3 value approximately fits the angular dependence of the collision probability obtained from our Monte Carlo simulations.

We propose a fitting formula of the form:

$$P_{col}(L_j/L_{12},\alpha) = \left\{ \left[0.07 \left(\frac{L_j}{L_{12}} - \frac{1}{2} \right) \right]^{-4} + 17500 \right\}^{-1/4} \left(\frac{\alpha}{10^{\circ}} \right)^{1.3}, \quad (1)$$

which has an initially linear growth for $L_j/L_{12} > 1/2$, and goes to a constant value for $L_j/L_{12} >> 1$. The p vs. L_j/L_{12} curves obtained for $\alpha=2.5,\ 5,\ 10$ and 15° are shown in Figure 1, showing a reasonable agreement with the results of the Monte Carlo simulations.

3. Collisions in a system of $N_i > 2$ outflows

We now consider a system of N_j identical biconical jet/counterjet systems with the same half-opening angle α and length L_j (from the source to the end of the cones). We assume that the outflow sources (at the tips of the cone pairs) are uniformly distributed within a sphere of radius R_c .

For a uniform, spherical distribution of sources with radius R_c , the average separation between source pairs is $\approx 1.03\,R_c$ and the root mean square separation is $\approx 1.09\,R_c$. We therefore assume that the average probability p_c for a collision between jet pairs is given by the following equation: (1) with $L_{12}=R_c$. This approximation of taking the same probability for the interactions of all outflow pairs is, of course, correct for the case of $L_j/R_c\gg 1$, for which the interaction probability does not depend on the separation between the outflow sources.

We now consider a set of Bernoulli experiments consisting of the success/failure events (with success probability P_{col} , see above) of the interaction between a given outflow i (with $i=1 \rightarrow N_j$) with an outflow j (with j having the N_j-1 values of the remaining sources). If the processes follow a binomial distribution, the expected number of collisions is

$$N_{col} = (N_i - 1)N_i P_{col}/2,$$
 (2)

with a standard deviation $\sigma = \sqrt{(1 - P_{col})N_{col}} \approx \sqrt{N_{col}}$ (the second equality being appropriate for $P_{col} \ll 1$).

Equation (3) is obtained for a binomial statistical distribution. When N_c approaches N_j , a more complex hypergeometric distribution should be considered. We do not study this limit because a real system of outflows with many jet interactions defies our simple picture of a system of biconical, geometrically fixed structures.

Now, combining equations (1) (with $L_{12} = R_c$) and (2) we obtain:

$$N_{col} = (N_j - 1)N_j \times$$

$$\left\{ \left[0.07 \left(\frac{L_j}{R_c} - \frac{1}{2} \right) \right]^{-4} + 17500 \right\}^{-1/4} \left(\frac{\alpha}{10^{\circ}} \right)^{1.3} / 2.$$
(3)

This is the expected number of jet collisions for a system of N_j conical bipolar outflows of half-opening angle α and length L_j from sources distributed within a radius sphere R_c . The standard deviation of the number of collisions with respect to this expected value is $\sigma \approx \sqrt{N_{col}}$.

Numerical experiments of systems of many biconical outflows

We now carry out experiments in which we randomly place N_j outflow sources within a sphere of radius R_c , also choosing a random outflow direction for each source. We then place biconical outflow structures of half-opening angle α and length L_j (for each of the cones) at the randomly chosen positions and directions. Finally, in the resulting structure, we count the regions of superposition of the outflow cones.

An example of a system with $N_j=5$, $\alpha=10^\circ$ and $L_j=3R_c$ is shown in Figure 2. The projection on the xy-plane of the 3D outflow cone structure is shown in green. This experiment has produced $N_{col}=3$ interaction regions (i.e., regions of cone superposition), as shown in white in Figure 2.

There is, of course, a larger number of "projected crossings" between the outflow cones, which do not correspond to physical interactions. Looking in the green structure of Figure 2, one counts approximately $N_{proj} = 7$ regions in which the projected cones cross each other (some of these regions being superpositions of more than two cones). A general result in all the multi-jet experiments that we have run have that $N_{proj} \sim 0.5 \rightarrow 2N_j$. We do not find any clear trends with the opening angle or with jet length for $R_i/R_c > 1$.

The number N_p of collisions counted in a series of experiments (a single experiment for each choice of N_j , α and L_j/R_c) are shown in Figure 3:

- the top frame shows N_p as a function of the half-opening angle α of experiments with $N_j=10$ and $L_j/R_c=1$ (blue crosses), and 3 (red dots). The results obtained from equation (3) for the appropriate values of α and N_j are shown with the solid red (for $L_j/R_c=3$) and blue $(L_j/R_c=1)$ curves. The dashed curves represent the $\pm \sigma$ curves of the theoretical N_{col} (see equation 3),
- the bottom frame shows N_p as a function of the number of outflows N_j for experiments with $\alpha=5^\circ$ and and $L_j/R_c=1$ (blue crosses) and 3 (red dots). The red and blue curves are the corresponding analytic predictions obtained from Eq. (3).

5. A gasdynamic simuation

Using the "yguazú-a" adaptive grid, gasdynamic code (Raga et al. 2000), we have computed a simulation of a system of five initially conical, bipolar outflows. The jets are identical, with an $\alpha=10^\circ$ opening angle and a $L_0=4\times10^{16}$ cm initial length. A constant $n_j=1000~{\rm cm}^{-3}$ density, $T_j=1000~{\rm K}$ temperature and $v_j=100~{\rm km\,s}^{-1}$ radially directed velocity is re-imposed within the inner part of the cones (of length $L_0/2$) after each computational time

step. The environment is initially at rest, with a homogeneous $n_a = 1 \text{ cm}^{-3}$ density, and $T_a = 1000 \text{ K}$ temperature.

For the jet source positions and outflow directions, we have chosen the randomly sampled position/direction combinations of the $N_j=5$ model, as shown in Figure 2. For the gasdynamic simulation, we have assumed that the source positions are sampled within a $R_c=5\times 10^{16}$ cm sphere, in the center of computational domain.

The simulation is done in a Cartesian grid with an extent of 2×10^{17} cm along the 3 axes, using a 4-level binary adaptive grid with a maximum resolution of $\approx 3.9\times 10^{14}$ cm (corresponding to 512^3 cells at this resolution). Outflow conditions are applied to all grid boundaries.

The gas is assumed to be initially neutral (in the jet cones and in the environment), except for a small seed ionization fraction that feeds the collisional ionization cascade. A rate equation for neutral Hydrogen is solved together with the gasdynamic equations, and the parametrized cooling function of Raga et al. (2002) is included in the energy equation, as follows:

Figure 4 shows a time-series of column density maps (integrated along the *z*-axis) obtained from the simulations. The initial outflow cones (top frame) expand almost freely in the low density environment (other two frames of Figure 4), and produce many lines of sight superpositions and two visible jet interaction regions.

At t=400 yr, the jet cones have reached a length of $\approx 1.6 \times 10^{17}$ cm $\approx 3R_c$ (where R_c is the outer the radius of the sphere containing the outflow sources, see above). Therefore, the bottom frame of Figure 4 can be directly compared with the cone pattern of the geometric outflow model of Figure 2 (note that Figure 2 covers twice the physical domain of Figure 4).

From this comparison between Figures 2 and 4, it is clear that the geometric and gasdynamic models share the same distribution of outflow orientations and source positions. Looking at the geometric model of Figure 2, we see that this configuration of outflows have three superposition regions (in white):

- The upper one is seen as a major jet collision in the numerical simulation, resulting in a dense, approximately interaction region in which the two colliding cones are redirected in an approximately vertical direction (see the bottom frame of Figure 4).
- the lower cone superposition region also appears as a dense two-jet interaction region in which part of the interacting cones are redirected to the bottom right direction,
- the central, small cone superposition region (see Figure 2) can be seen as a column density peak (in the bottom frame of Figure 4), but does not produce a major redirection of the impinging jets.

Therefore, two of the three cone superposition regions were observed in the numerical simulation, and there were major disruptions in the colliding outflows. The third cone superposition of our distribution of outflows is only a grazing collision involving only a part of the cross-sections of the colliding jets.

6. Application to observed outflow systems

Let us assume that we have an image of a system of N_j bipolar outflows. We can then calculate:

- the mean tangent of the half-opening angle $\overline{\tan \alpha_p}$ of the projected cones,
- the mean length \overline{L}_p of the jets (measured from the sources to the tip of one of the outflow lobe),

• the root mean square separation $\overline{\Delta R}$ between all possible source pairs.

If we assume that the jets have the same intrinsic length, for a random direction distribution of the outflows, we can estimate the true (un-projected) half-opening angle α of the outflows through:

$$\tan \alpha = 0.59 \, \overline{\tan \alpha_p} \,, \tag{4}$$

and the true (unprojected) length of the jets as

$$L_i = 1.70 \, \overline{L}_p \,. \tag{5}$$

Also, if we assume that the source positions are randomly distributed within a spherical volume of radius R_c . we can estimate this radius through:

$$R_c = 0.92 \, \overline{\Delta R} \,. \tag{6}$$

As an illustration of how this method can be applied to an observed system of outflows, we apply it to the NGC 1333 region. Davis et al. (2008) showed that this region has a number of superimposed outflows (see Raga et al. 2013). If we consider the outflows from the YSO 15, 18, 20, 22 23 and 32 sources (with 2 outflows arising from the YSO 23 source), we have a system of $N_j=7$ outflows. Considering a distance of 220 pc to NGC 1333, from Figure 7 of Davis et al. (2008), we find a $\overline{\Delta R}=6.96\times10^{17}$ cm mean square separation between the outflow sources and a mean projected length $\overline{L}_p=1.48\times10^{18}$ cm for each outflow lobe.

Using equations (5-6) we obtain an estimated de-projected jet length $L_j=1.36\times 10^{18}$ cm and a radius $R_c=1.18\times 10^{17}$ cm, therefore obtaining $L_j/R_c\approx 0.87$. Now, $N_j=7$ and $L_j/R_c\approx 0.87$, from equation (3), we find:

$$N_{col} \approx 1.1(\alpha/10^{\circ})^{1.3}/2$$
. (7)

It is not straightforward to estimate the half-opening angle α of the NGC 1333 outflows. From the Spitzer image in Figure 4 of Raga et al. (2013), we estimate a mean half-opening angle $\alpha_p \approx 5^\circ$, which through equation (4) gives a deprojected $\alpha=3^\circ$ Inserting this angle in equation (7), we obtain $N_c \approx 0.11$, with a standard deviation of 0.34.

Therefore, for the NGC 1333 system, the expected number of physical collisions between the observed outflows is zero. This is only the statistically expected value, and there is a non-zero probability of actual collisions taking place.

The probability of a collision between two jets in NGC 1333 can be estimated as follows: consider the jets from YSO23 and YSO24 of Davis et al. (2008). The two outflow sources have a projected separation of $\sim 15''$, and their projected lengths are considerably longer if we use the projected separation and length as estimates of deprojected separation and length. We conclude that these two jets are in the "large L_j/L_{12} " regime of a two-jet interaction (see Figure 1). From equation (1), for $\alpha=3^\circ$ and $L_j/L_{12}\gg 1$ we obtain $P_{col}\approx 0.011$. This estimate tells us that there is a low probability of a few times ~ 1 % of having a jet collision between two given jets.

To complement our analysis, we examine a more massive and significantly denser star-forming environment, the Orion Nebula Cluster (ONC) (Kroupa et al. 2018). This region is known to host a significant number of young stellar objects (Alves & Bouy, 2012), most of which are likely to drive bipolar, collimated outflows. By applying the same statistical framework to Orion, we aim to

investigate the dynamic consequences and enhanced interaction rates resulting from a significantly higher stellar density.

We assume a system composed of $N_i = 10^4$ randomly distributed bipolar outflows, corresponding to the approximate number of young stars in the Orion cluster (Megeath et al., 2012). We adopt a typical intrinsic jet length of $L_i = 0.1$ pc and consider a spatial distribution confined within a spherical region of radius $R_c = 2$ pc, which roughly corresponds to the size of the central ONC core (Kroupa et al., 2018). For the intrinsic half-opening angle of the jets, we assumed a value of $\alpha = 3^{\circ}$, consistent with the observational constraints from collimated jets in young stars (Erkal et al., 2021). Using the full analytical formulation for the expected number of collisions (Equation 3), we find a collision probability of $P_{col} \sim 0.65\%$. Although the jet-jet collision probability is low, each individual jet is expected to experience approximately 66 interactions on average. This outcome illustrates the combinatorial amplification effect: even a small probability, when considered over a large ensemble of jets, results in a substantial cumulative effect on the cluster's dynamical evolution.

We can also increase the half-opening angle to $\alpha=10^\circ$, while keeping $L_j/R_c=0.05$, which results in a substantial rise in the expected probability of collision: $P_{col}\sim3.14\%$, leading to an average of 314 collisions per jet. This parameter variation demonstrates that, although changes in jet length and cluster size moderately affect interaction rates, variations in the angular width have the most dominant effect, dramatically enhancing the probability of jet-jet interactions in dense star-forming environments.

In the case of Orion, we chose to focus on reporting the average number of collisions per jet rather than the total number of collisions. This choice is motivated by the fact that our analytical framework does not impose a limit on jets that have already interacted, implicitly treating each possible pairwise interaction as independent, even after multiple encounters. In other words, the model assumes that once a jet interacts, it remains geometrically and dynamically available for further interactions as if no physical alteration has occurred. As discussed in § 3, when the total number of collisions becomes comparable to the total number of jets, a more complex hypergeometric distribution is required to accurately capture the statistics. We do not explore this limit here, as a real system of outflows with many mutual interactions would defy our simplified picture of geometrically fixed biconical structures.

6.1. Volume filling factor

An important consideration that emerges from this statistical framework is the connection between the number of outflow interactions and the fraction of the volume evacuated by jets. Because each bipolar outflow traces a biconical volume, the cumulative effect of many such jets is to fill a significant portion of the host cluster's volume. Once a critical fraction is filled, the geometric overlap between outflows becomes statistically inevitable. A useful quantity for describing this collective effect is the volume filling factor, which is defined as the fraction of the cluster volume dynamically influenced or occupied by the jets at a given time.

The volume of a single bipolar outflow was approximated as the sum of two identical cones. The instantaneous volume cleared by a single bipolar jet is thus given by:

$$V_{jet}(t) = 2 \times \frac{1}{3}\pi L_j(t)^3 \tan^2 \alpha$$
 (8)

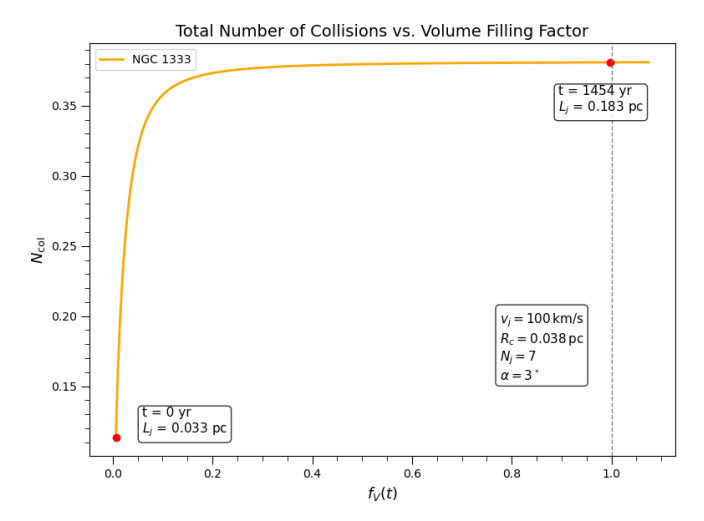


Figure 5. Total expected number of jet-jet collisions, N_{col} , as function of the volume filling factor, $f_V(t)$, for the NGC 1333 region. The curve corresponds to a system of $N_j=7$ bipolar outflows, each with an initial jet length of 0.033 pc, confined within a spherical cluster of radius $R_c=0.038$ pc, and adopting a half-opening angle of $\alpha=3^\circ$. The initial and final points are indicated in red. The dashed vertical line marks the point where the volume filling factor reaches unity ($f_V=1$), indicating that the jets fully occupy the cluster volume. The text boxes indicate key physical parameters, including the jet velocity, characteristic scales, and corresponding jet lengths at the initial and final times. This graph illustrates how collision rates increase as the jets dynamically expand and progressively fill the available volume.

where $L_j(t)$ is the instantaneous jet length and α is the intrinsic half-opening angle of each cone. When considering a total of N_j jets randomly distributed within a spherical region of radius R_c , the total evacuated volume is expressed:

$$V_{tot}(t) = N_i \times V_{jet}(t). \tag{9}$$

We then define the volume filling factor as:

$$f_V(t) = \frac{V_{tot}(t)}{V_c},\tag{10}$$

where $V_c = \frac{4}{3}\pi R_c^3$ denotes the total volume of the cluster region under consideration. In this case, the volume filling factor simplifies to:

$$f_V(t) = \frac{N_j L_j(t)^3 \tan^2 \alpha}{2R_c^3}.$$
 (11)

This expression reveals that the volume filling factor depends cubically on the jet length and quadratically on the opening angle, thereby embedding direct information about both the jet dynamics and geometry. As jets grow over time during the YSO evolution phase, the volume filling factor tends to increase, indicating the progressive occupation and dynamical influence of the outflows within the cluster volume. Physically, $f_V(t)$ quantifies the fraction of the cluster volume that is dynamically influenced or evacuated by the jets at a given time. When the volume filling factor is small, jets remain mostly isolated, and interactions are rare; as approaches unity, the system transitions into a highly interactive regime, where overlapping cavities and mutual collisions become increasingly probable.

7. Conclusions

A simple model for interaction in a system of identical conical bipolar outflows is presented. We first compute (with a Monte Carlo approach) the probability of having a collision between two outflows.

As expected, the probability P_{col} of having an interaction (which corresponds to a partial superposition of the outflow cones in our simple geometric model) is a function of their half-opening angle α and of the ratio L_j/L_{12} between the length of the outflow lobes and the separation between the outflow sources. As expected, we find that $P_{col}=0$ for $L_j/L_{12}<1/2$ and also a $P_{col}\to P_{\infty}(\alpha)$ for $L_j/L_{12}\gg 1$. This behavior is shown in Figure 1. We find an analytic fit for $P_{col}(L_j/L_{12},\alpha)$ (see § 2 and Figure 1).

Building upon this, the derived interaction probability for two-outflows is used to estimate the expected number of jet interactions in a system composed of $N_j > 2$ identical outflows (see § 3). Assuming that the interactions follow a binomial distribution (as appropriate for a system with only a few jet interactions), we then derive an analytic expression (equation 3) for the expected number of jet collisions for a system of bipolar jets with random directions ejected from N_j sources that are uniformly distributed within a spherical "cluster" of radius R_c . The result is a simple analytic expression giving the expected number N_c of two-jet collisions as a function of the half-opening angle α of the outflow cones and the jet length to cluster radius ratio L_j/R_c (see Eq. 3).

Additionally, a series of Monte Carlo simulations were carried out for systems of $N_j=5\to 25$ identical outflows with half-opening angles $\alpha=2\to 15^\circ$ and lengths $L_j=(1,3)\times R_c$, with which we checked our analytic estimate for the expected number N_c of outflow collisions, which we derived analytically (Eq. 3). A satisfactory agreement is obtained between the Monte Carlo simulations and the analytical $N_c(L_j/R_c,\alpha)$ (see Figure 3).

To explore the properties of systems of interacting jets beyond our simple biconical outflow geometric model, we carried out a single 3D gasdynamical simulation of a system of five initially biconical outflows. For the chosen configuration of the source positions and outflow directions, the geometric model gives three "cone superposition" regions (Figure 2). Two of these superposition regions are seen as the major two-jet interactions in the gadynamical simulation, with high compressions and substantial redirection of the interacting outflows (see Fig. 4). The third cone superposition region (of the geometric model, see Figure 2) is observed as a minor grazing collision in the gasdynamical model (see Figure 4).

Finally, we describe how to calculate the expected number N_c of two-jet collisions in a system with N_j outflows. We propose calculating the root mean square of the projected separations between the outflow sources to estimate the physical radius R_c of the region in which the sources are distributed. In addition, the mean projected length of the jets can be used to estimate the (deprojected) average jet length. Finally, the half-opening angle α must be estimated from the observations (deprojecting the observed, projected opening angles of the outflows).

With the resulting observational determinations of N_j , α and L_j/R_c , one can use equation (3) to calculate the expected number N_c of two-jet collisions in the observed outflow system. We illustrated this procedure using published observations of the NGC 1333 outflow system.

When trying to obtain the parameters necessary for calculating N_c (through Eq. 3), the half-opening angle α is the most uncertain.

It is unclear where the edges of the outflow lobes are and whether one must consider a more central jet-like component or the broader envelope seen in some outflows. Given this difficulty, it is possible to appropriately invert equation (3) to obtain the opening α angles necessary for obtaining $N_c \ge 1$.

In this study, we derived a relatively simple method to estimate the expected number of two-jet collisions in a system with many outflows. Its application to many observations is possible.

It is important to emphasize that the statistical estimates derived here rely on the assumption that the outflow sources are randomly distributed throughout a cluster volume and that the jet orientations are isotropic. However, in real star-forming regions, the distribution of young stellar objects is often non-uniform. Stellar clustering, filamentary gas structures, and the high prevalence of binary and multiple systems introduce significant spatial correlations among sources. These effects are expected to increase the probability of jet-jet interactions, particularly in compact binaries or small groups, where the projected separations are small. Consequently, the number of physical overlaps estimated under the uniform distribution assumption should be considered as a lower limit. More realistic models that account for stellar multiplicity and substructures may yield higher collision probabilities.

Dr. Alejandro Raga, the lead author of this study, passed away on July 20, 2023. A couple of weeks prior, the co-authors provided final comments to update the manuscript before submission. The authors thank Pablo Velázquez and Ary Rodríguez (Instituto de Ciencias Nucleares) for their help in recovering Dr. Raga's files

related to this work. Dr. Raga was an amazing friend and an excellent colleague. He will be fondly remembered and missed.

This work was supported by the DGAPA (UNAM) grants IG100422 and IN110722.

■ REFERENCES

Alves, J., & Bouy, H. 2012, A&A, 547, A97, doi: 10.1051/004-636 1/201220119

Davis, C. J., Scholz, P., Lucas, P., Smith, M. D., & Adamson, A. 2008, MNRAS, 387, 954, doi: 10.1111/j.1365-2966.2008.13247.x
Erkal, D., Deason, A. J., Belokurov, V., et al. 2021, MNRAS, 506, 2677, doi: 10.1093/mnras/stab1828

Kroupa, P., Jeřábková, T., Dinnbier, F., Beccari, G., & Yan, Z. 2018, A&A, 612, A74, doi: 10.1051/0004-6361/201732151

Lefloch, B., Gusdorf, A., Codella, C., et al. 2018, A&A, 581, 4, doi: 10.1051/0004-6361/201425521

Megeath, S., Gutermuth, R., Muzerolle, J., et al. 2012, AJ, 144, 192, doi: 10.1088/0004-6256/144/6/192

Nony, T., Motte, F., Louvet, F., et al. 2020, A&A, 636, A38, doi: 10 .1051/0004-6361/201937046

Raga, A. C., de Gouveia Dal Pino, E. M., Noriega-Crespo, A., Mininni, P. D., & Velázquez, P. F. 2002, A&A, 392, 267, doi: 10 .1051/0004-6361:20020851

Raga, A. C., Navarro-González, R., & Villagrán-Muniz, M. 2000, RMxAA, 36, 67

Raga, A. C., Noriega-Crespo, A., Carey, S. J., & Arce, H. G. 2013, AJ, 145, 28, doi: 10.1088/0004-6256/145/2/28

Zapata, L. A., Fernández-López, M., Rodríguez, L. F., et al. 2018, AJ, 156, 239, doi: 10.3847/1538-3881/aae51e